Modeling and Simulation of RF MEMS devices

RAJESH S. PANDE, RAJENDRA M. PATRIKAR
Department of Electronics and Computer Science
Visvesvaraya National Institute of Technology
NAGPUR
INDIA
panderaj@yahoo.com, Rajendra@computer.org

Abstract: - A stable, device specific, multiple energy domain and multi scale simulation tool for Radio Frequency (RF) MicroElectroMechanicalSystems (MEMS) devices is developed. A structured design methodology is adopted for design and optimization of RF MEMS shunt switch and MEMS inductor. The Computer Aided Design (CAD) tool incorporates physical parameters such as surface roughness. An electro-mechanical model of the RF MEMS shunt switch is solved by a numerical technique based on the iterative Finite Element Method (FEM). The electrical properties such as capacitance and electric field are obtained. The algorithm to extract inductor is based on solution of Laplace equation by FEM followed by current density computation. The energy of resulting magnetic field is estimated by Monte Carlo sampling. The tool also generates CIF (Caltech Intermediate Form) net list necessary for planar mask lay out. The tool analyzes the impact of surface roughness and also does thermal analysis. These are useful for understanding reliability and failure mechanisms of RF MEMS components.

Key-Words: - RF, MEMS, CAD, EDA, FEM, surface roughness

1 Introduction

The advent of VLSI-compatible MEMS fabrication technologies has led to the development of increasingly complex and integrated MEMS based systems. In parallel with the development of new technologies, new device configurations, and new applications for MEMS devices and systems, there is a growing need for computer-aided engineering and design systems. As product volume grows and as the time-to-market becomes more crucial, there will be an increasing need for effective modeling and simulation tools that permit experimentation before costly fabrication. In MEMS CAD significant progress has been made, but the current state-of-the art tools have not yet achieved the maturity what CAD tools have for VLSI (Very Large Scale Integration). Most MEMS CAD tools are focusing on device level characteristics. The commercial CAD systems for MEMS design are generic in nature. Hence the available CAD tools are lacking ability to predict design performance and optimization with regard to some of the parasitic effects. For example most of the surfaces are represented by smooth topologies and in reality most of the surfaces are rough. There are other parameters such as noise is also not accounted in generic tools [1]. It is necessary to take into account these surface properties since surface to volume ratio is increasing for all devices as the dimensions are continuously shrinking. The accurate modeling of the physical properties such as surface topology and its impact on the electrical parameters will help to predict the deviation in performance. For example it is reported that rough surface contact formed between the bridge metal and the isolation layer in the "down" position of the capacitive coupled switches may lead to the discrepancy between the measured and predicted data as high as 40% since the technology is in the inception stage [2] [3]. The device designer needs to understand the device performance with the help of accurate modeling and simulation of device model. This is essential to improve the manufacturability of MEMS devices as seen in silicon technology. The tools are also lacking support to testability. The CMOS circuit technology works mainly in electrical domain as oppose to MEMS devices which have different domains based on the application. Thus it may be necessary that for each MEMS device specialized CAD tool is required, which takes into account all the domain characteristics. The recent efforts in microelectronics and MEMS have shown promising results in realization of high-performance passive components for RF applications. However, modeling and simulation of MEMS RF components is quite challenging because of complexity involved. CAD systems for MEMS require three dimensional modeling to take into accounts all the domain characteristics. In the today's technology, computing electrical parameters such as inductance or capacitance using conventional techniques is no longer accurate because of miniaturization. At the same time, using highly accurate techniques such as a fine-grained Finite Element Method may not be feasible due to the large computation time. Our efforts are focused to develop the tool for RF MEMS shunt capacitive switch and MEMS inductor considering some parasitic effects such as roughness. The mechanical analysis of RF MEMS shunt switch is performed by creating FEM model of the structure.

One of the major problems with any electronic component today is long term reliability of the device particularly at the inception stage. The RF MEMS devices have demonstrated outstanding performance with regard to near to zero static power dissipation, high quality factor and better noise figure, so now the lifetime characterization of these devices is essential. To study reliability issues, the failure mechanism of these devices must be understood. The primary failure of RF MEMS capacitive shunt switch is due to stiction. The stiction occurs due to the dielectric charging of silicon nitride layer. The dielectric charging of silicon nitride layer takes place due to Frenkel-Poole mechanism. The Frenkel-Poole mechanism depends on electric field and temperature. The electric field increases with roughness and affect reliability of switch. The radio frequency waves flowing through switch generates heat due to dissipation in side walls. The temperature rise increases the dielectric charging mechanism. The temperature distribution inside the switch helps analysis of failure mechanism. This tool also analyzes the temperature distribution in the structure.

2 CAD Framework for RF MEMS design

The MEMS-device designer requires an accurate, behavior model that captures all the essential behavior, including parasitic effects and permit predictable design modifications and optimizations. The Rapid, accurate, efficient analysis of many alternatives during the design process is crucial to developing high quality, robust devices and systems. MEMS are miniature electromechanical systems developed from the mature batch-fabricated processes of VLSI technologies. Typical components of CAD framework are 3-D and 2-D visualization of structure and parameters, graphical user interface (GUI) for entry of devices, numerical analysis, statistical analysis and display of calculations. In case of MEMS, numerical electrical as well as mechanical analysis is required. In developing the MEMS design tool, the design process can be considered as combination of EDA (Electronic Design Automation) and MDA (Mechanical Design Automation). The EDA covers partial derivative equations physics solvers, layout and process tools and spice. The MDA includes solid modeling and mesh generation tools, partial derivative equations physics solvers in mechanical domain. The integration of EDA and MDA must also support new design methodologies. Commonly used MEMS design methodology is unstructured design flow. Lack of hierarchy and one-way design flow are the main drawbacks of this methodology. The advantages of structured design approach are reusability of the parametric circuit models and allow quick iteration between system, circuit and layout representations. The structured design environment provides the usability of technology to large scale fabrication. The structured design approach has significantly contributed to the explosive growth of VLSI technology. MEMS design methodologies in wide use today, do not support hierarchical representations suitable for verification based iterative systems. This methodology adopted from the electronic design techniques enables fast design verification of complex electronic and micromechanical designs [4][5][6]. Complexity in electronic design is handled through a hierarchy of devices, components and blocks, which can share the same layout representation. EDA tools support this design hierarchy. Due to uniform nature of representation, the designer can use various levels of abstraction. It also helps to make the iterative design process faster. Due to mixed energy domains the MEMS have greater complexity. The generic design flow for MEMS is shown in Fig. 1 [1][4][7][8]. In the design flow of Fig. 1, since the tool developed is intended for RF MEMS shunt switches and MEMS inductors only, the technology information is passed to schematic and simulation blocks.

The information related to the parasitic effects also should be provided. In generic tools, the component library is available. The design rule constraints and process are of CMOS micromachining process.

The RF MEMS devices are fabricated using custom VLSI processes with Silicon, Aluminum, polysilicon and Silicon nitride. For a given fabrication technology, CAD tools are essential for creating the physical parts.

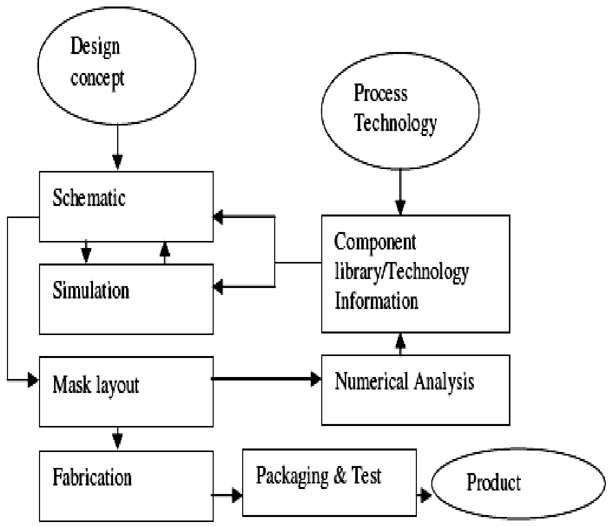

Fig. 1 Generic design flow for MEMS

Usually, the final output of CAD system of VLSI CAD tools are mask layouts used in lithographic processes, which is also true for MEMS CAD program.

The tool developed, fits into framework illustrated in the Fig. 1. The tool is aimed at RF shunt switch and RF MEMS inductor only and thus all the individual modules are developed for these devices only.

The tool uses three-dimensional geometry. The visualization program is developed in OpenGL (Open Graphics Library) [9]. OpenGL is the premier industry standard, stable environment for developing portable, interactive 2D and 3D graphics applications. OpenGL is one of the most widely used and supported 2D and 3D graphics application programming interface. It is a software interface to graphics hardware. OpenGL promotes innovation and speeds application development by incorporating a broad set of rendering, texture mapping, special effects, and other powerful visualization functions. It gives software developers access to geometric and image primitives, display lists, modeling transformations, lighting and texturing, anti-aliasing, blending and other features. This interface consists of distinct commands that can be used to specify the objects and operations needed to produce interactive three-dimensional applications. OpenGL is designed as a streamlined, hardware-independent interface to be implemented on many different hardware platforms. One can build desired model from a small set of geometric primitives, points, lines, and polygons. A sophisticated library that provides these features could certainly be built on top of OpenGL. The OpenGL Utility Library (GLU) provides many of the modeling features. The schematic of RF MEMS shunt multiple supported switch, cantilever switch, RF MEMS inductor using the OpenGL library is developed. The three-dimensional meshed models are developed by the tool. The solid models can be used for various mechanical and electrical analyses. The tool is also useful for visualization of geometries and has 3-D solid modeling capability. The 3D visualization offers RF MEMS designers a platform for immediately visualizing devices for desired fabrication process without having to wait for the actual fabrication. It enables the designer to see the interaction of different layers of the process being used. It is especially useful in viewing 3-D, out-of-plane, multi-degree-of-freedom RF MEMS structures.

With the ability to manipulate the structures in a three-dimensional environment, this package becomes a design checker for undesired hinge binding and travel stops. Thus it becomes an important part of designing movable, out-of plane structures. The important aspect of this type of tool is to construct the model for mechanical and electrical analysis. Besides this visualization is important part of such tool. The micromechanical analysis is performed by creating Finite Element Model of the structure. Numerical analysis includes the meshed device model and solving FEM equations. FEM is a powerful and versatile numerical technique for handling problems involving complex geometries and inhomogeneous media. The FEM is also used here for calculating the electrical parameters such as node voltages in this tool. The tool converts the schematic into mask layout in CIF format. Layout follows design rules of conventional CMOS processes. The CIF net list necessary for planar mask lay out and geometry files are generated by the tool from schematic. The CIF file generated includes information regarding layers and 2D geometrical dimensions. The CMOS fabrication process accepts the CIF file to build masks. CIF files can be converted into GDS files, which are industry standard by many good quality tools.

3 Modeling of RF MEMS shunt switch

MEMS switches can be used in a variety of RF applications, including cell phones, phase shifters, and smart antennas, as well as in lower frequency applications, such as automatic test equipment

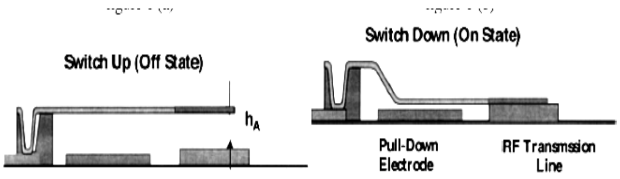

Fig. 2 Cantilever RF MEMS switch

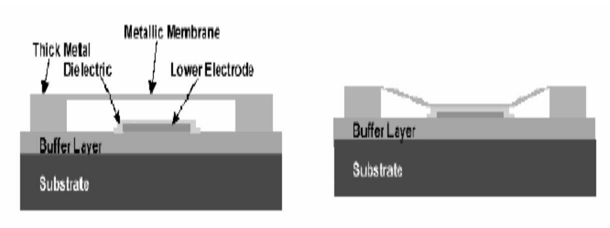

Fig. 3 RF MEMS shunt switch (Multiple supported)

(ATE) and industrial and medical instrumentation. MEMS switches are receiving increasing attention, particularly in the RF community. Low power consumption, low insertion loss, high isolation, excellent linearity, and the ability to be integrated with other electronics make micro switches an attractive alternative to other mechanical and solid-state switches. Furthermore, MEMS switches have lower off-state capacitance and, as a result, better off-state RF isolation than either FETs or PIN diodes. MEMS switches have inherently high RF linearity. Intended applications include microwave switches that replace PIN diodes and FET switches, while providing lower insertion loss, higher isolation, higher linearity, higher radiation resistance, superior tolerance for high temperature environments, and lower prime power consumption. Examples of such applications include transmitter and receiver (T/R) switches in a variety of products, such as cellular handsets and base stations, phase shifters for electronically steer able antennas, tunable filters, and reconfigurable antennas [10]. Example shown here is of MEMS shunt switch. Radio Frequency (RF) MEMS shunt switches offer significant improvements over their macro scale counterparts. These switches exhibit low insertion loss (0.2 dB at 35 GHz) with good isolation (35 dB at 35 GHz). These devices possess on–off capacitance ratios in the range of 75 to 110 with a cutoff frequency in excess of 9000 GHz. The RF MEMS shunt switches are considered here because of their practical utility. The Cantilever switch shown in Fig. 2 (b) and multiple supported air bridge shown in Fig. 3 are the two common RF MEMS shunt switch structures [11] [12] [13]. The tool developed here represents these switches as shown Fig. 4 (a) (b). The capacitive coupling switches have a thin dielectric film and an air gap between the two metallic contact surfaces. The air gap is electromechanically adjusted to achieve a capacitance change between the 'up' (Off) and 'down' (On) state.

The switches have a movable metal membrane (Aluminum alloy), which pulls down onto a metal/dielectric (Silicon Nitride) sandwich to form a capacitive switch. A typical RF capacitive MEMS switch shown here has 120-µm width, 280-µm length, air gap in the switches 2 µm, the insulator thickness 0.1 µm and its dielectric constant 7 which is presented by Yao [13].

A mechanical FEM model of the RF MEMS switch is adopted to predict the effects of movement in high switching speed applications [14][15]. For mechanical modeling of RF MEMS shunt switch, Finite Element Analysis (FEA) model is developed. When the voltage is applied between the lower electrode and the metal membrane, the membrane is subjected to the electrostatic force, retaining force of spring and the viscosity force due to the presence of air. The tool generates grid i.e. divides the solution region into finite number of sub regions or elements.

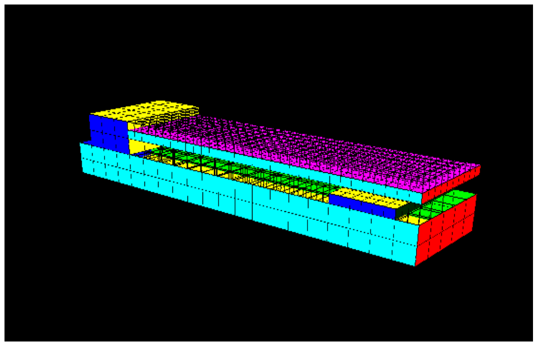

Fig. 4 (a) Meshed model of Cantilever MEMS switch

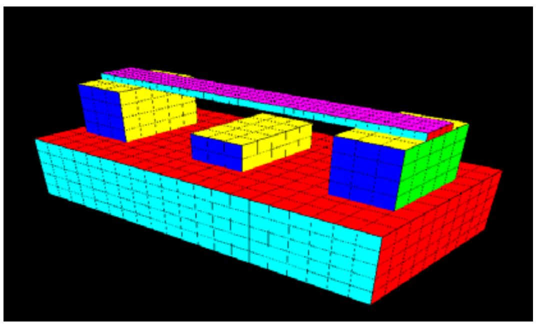

Fig. 4(b) Meshed model of RF MEMS shunt switch (Multiple supported)

If a long body of uniform cross section is subjected to transverse loading along its length, a small thickness in the loaded area, then the problem can be modeled as plane strain. The metal membrane exhibits plane strain conditions. The solution region i.e. membrane is divided into 672 triangular elements. Governing equation for a typical element are evaluated. The interpolation polynomial is $\varphi(x,z)=a_1 + a_2 x + a_3 z$, considering the membrane in x-z plane and force applied in x-y plane. The stress-strain relationship is dictated by Hooke's law $[\sigma] = [D]\,[\varepsilon]$, where $[\sigma]$ is stress matrix, $[\varepsilon]$ strain matrix and [D] is matrix of material characteristics. For plane strain conditions

$$[D] = \frac{E}{1+\mu}\begin{bmatrix} d & b & 0 \\ b & d & 0 \\ 0 & 0 & 1/2 \end{bmatrix}$$

where $d = (1-\mu)/(1-2\mu)$, $b = \mu/(1-2\mu)$, μ = Poisson's ratio

E = elastic modulus of membrane

The element connectivity information which shows the correspondence between local and global numbers is generated. The linear shape functions are defined, which are used in interpolating the displacement field. Galerkin's formulation is adopted to solve the problem. The governing equations for plane strain problem are obtained. The element coefficient matrix $[K^e] = [B]^T [D] [B]\, t\, A$. The matrix [B] is element strain-displacement matrix. The element area is A and t is thickness of element, 'unity' for plane strain condition. The element coefficient matrix is evaluated. The structural global coefficient matrix is obtained from element coefficient matrices using the connectivity table. The degree of freedom of all nodes is taken into consideration. The electrostatic force on the metal membrane is calculated. This force depends on the distance between membrane and bottom electrode, in other words depends on the capacitance of the switch. The electrostatic force due to actuation voltage deflects the membrane. This initial displacement further increases the electrostatic force. Increased force attracts the membrane further causing more displacement. As the membrane go down the capacitance increases resulting in increased force after iteration. For the applied potential of 30V the membrane is pulled down. When the applied potential is removed, the membrane goes up. The time required for pull down is large compared to pull up. The maximum possible displacement of the membrane is 2 μm. The maximum displacement along degree of freedom is specified, which gives boundary conditions. By introducing variable capacitance in a non-linear circuit solver, the switch performance in terms of distortion can be evaluated. By iteration method the solution is obtained. It is observed that the portion of membrane above electrode touches the dielectric uniformly. Thus the grid is used to calculate stiffness matrix for analyzing strain and other mechanical parameters. The element stresses, element nodal displacement vector can be obtained and analyzed with the tool developed. The differential equation describing the movement is given by [14]

$$-\frac{1}{2}\frac{V^2\varepsilon_0\varepsilon_r S}{\left[\delta(1/\varepsilon_r - 1) + x\right]^2} - k(x - x_0) - \gamma\dot{x} + \left(e^{-[\alpha(x-\delta)]^{\beta}} - 1\right)u(\delta - x) = m\ddot{x} \quad \text{.......... (1)}$$

where in Eq (1), ε_r is relative dielectric constant of Silicon Nitride, δ is the thickness of the dielectric, V is applied switching voltage, k is spring constant, m is membrane mass, γ is the air viscosity, parameters α and β determines the steep of the variation of the repulsive force as function of position, x is the displacement of membrane. The step function u(x) ensures that the repulsive force occur only when the plate penetrate the dielectric layer. The solution of Eq. 1 enables to calculate the time varying capacitance of the switch. The tool developed is validated by changing the distance between electrode and membrane. The electrostatic potential required to pull down the membrane changes.

The surface topography is modeled by the scale independent concept of self-similar fractals, which generates the rough surface. The fractal dimension describes the surface roughness and this method is found to be most suitable for surfaces in silicon. The rough surface is modeled using the Mandelbrot-Weierstrass function described by the following equation [16] [17].

$$f(x) = \sum_{n=-\infty}^{n=\infty} b^{-n(2-D)}\left[1 - k\cos(b^n x + \phi)\right] \quad \text{............... (2)}$$

Fractal dimension, D= log (N)/log (1/r), r is the ratio of N parts scaled down from the whole, By varying D rough profile is generated. b is the frequency multiplier value. The parameter k can be used to alter the profile. By varying D and k any profile can be generated. The frequency multiplier b varies typically between 1.1 and 3.0. D is a non-integer value, varies between 1 and 2 and ϕ is a randomly generated phase. The parameter k can be used to alter the profile, usually fixed value of k = 1 and b = 2 are used since surfaces used in most of the technological applications are fairly regular. The electrical properties such as capacitance and electric field for various values of D are obtained [18] [19]. The capacitance affects insertion loss and isolation. The capacitance and electric fields are calculated by solving Laplace equation with the finite difference method. The electric field contours and maximum electric field etc obtained from the data. The effect of surface roughness on Off and On capacitances is shown in Fig.5. The increase in Off capacitance results in higher insertion loss. With the increase in $C_{ON,}$ isolation will be higher. To model the effect on electric field due to roughness, Lapalce equation is solved and two dimensional electric field contours are obtained. From this data maximum electric field is calculated. For various values of D, maximum electric field is calculated and plotted in Fig. 6. The maximum electric field will be one of the factors, which decide the maximum voltage that can be connected between bottom electrode and membrane. It should also be considered while deciding the minimum possible thickness of the dielectric. The maximum electric field will occur where geometry is very rough resulting in electric field crowding and/or if the distance between two plates becomes minimum because of protuberances. Thickness and strength of dielectric at this point decides reliability of the device rather than on overall bulk properties. The maximum electric field between two surfaces increases with increase in D, which is a measure of surface roughness [18]. The increase in electric field results into degradation in reliability although it may not suffer breakdown. The fractal dimension D represents the degree of roughness quantitatively. We have presented simulation data till D = 1.6, beyond this value, roughness and thereby values of capacitance and electric field increase rapidly. Due to process control such a high value of D is not expected for real surfaces in microelectronic devices. However, slight roughness can also add to the parasitic values and in today's complex integrated circuits this change should be taken into account to improve accuracy in parasitic extraction.

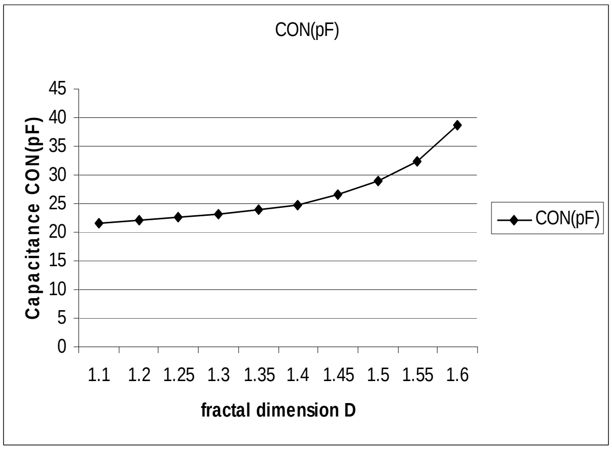

Fig. 5 (a) Effect of surface roughness on C_{ON}

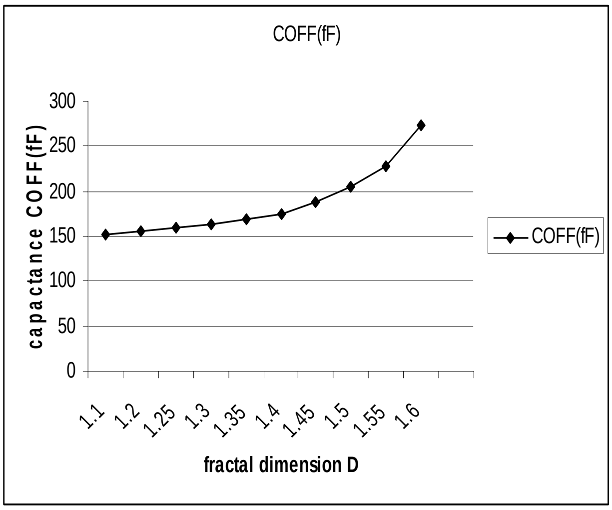

Fig. 5 (b) Effect of surface roughness on C_{OFF}

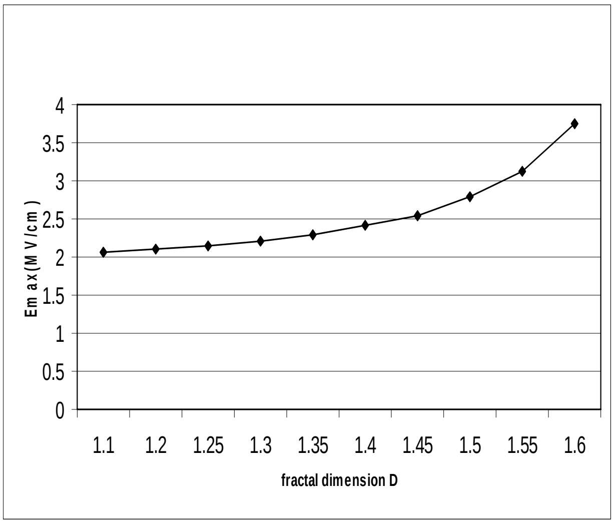

Fig. 6 Effect of surface roughness on maximum electric field

4 Thermal analysis of RF MEMS shunt switch

RF MEMS switches that can be integrated with existing technologies for high-speed electronics are an attractive proposition for variety of applications. However, before this technology can be inserted into mainstream systems, adequate reliability of the electromechanical devices must be demonstrated. The long-term reliability of MEMS switches is of major concern and is currently the subject of an investigation.

For capacitive switches, the primary failure mechanism is stiction between the dielectric layer and the metal. The stiction occurs due to dielectric charging within the switch Silicon Nitride layer which is used as dielectric [20]. The dielectric charging contributes to the failure of the bridge in the down-state position. The electric field can be as high as 3-5 MV/cm in the dielectric layer, which results in a Frankel-Poole charge injection mechanism from the metal to the dielectric resulting charge built-up in dielectric. The trapped charges within the dielectric tend to screen the applied electric fields that are used to control the actuation and release of the switch. The end result is that the screening voltage builds up within the dielectric and hinders operation of the switch. The trapped charges may provide enough potential to keep the membrane down since holding voltage is small than threshold voltage. This results in the switch being stuck down. It has been observed that the thermal heating due to RF power plays important role in the failure of RF MEMS shunt switches [21]. The effect of the RF power on the steady-state temperature of the switch and its effect on reliability of a capacitive MEMS shunt switch is analyzed. A typical RF capacitive MEMS switch shown in Fig. 3 is considered here for analysis. The switch has 120-µm width, 280-µm length and air gap in the switch is 2 µm, the insulator thickness is 0.1 µm and its dielectric constant is 7. The values of Coff and Con are 147 fF and 20.8 pF respectively. The main mode of heat transfer is due to conduction in the body of switch. The steady-state temperature distribution on a rectangular MEMS bridge is solved using the generalized heat conduction equation with constant thermal conductivity given by

$$\nabla^2 T + \frac{\dot{g}}{k} = 0$$

where T is the temperature of the MEMS bridge (degree Celsius), ***g*** is the rate of heat generated per unit volume (W/m^3), and ***k*** is the thermal conductivity of the bridge [22]. In the capacitive switch the microwave power induces current in the suspended bridge, which results in Ohmic heating. The power dissipated in the shunt switch is given by $P = (1/2)I^2_{rms}$ Rs, where Rs is the resistance of the bridge. The RF power dissipated in the switch in down-state is more than the power dissipated in up-state. It is shown that the temperature of the MEMS bridge does not follow the time-domain RF current. The steady-state analysis is therefore a valid assumption. The computer program developed solves 3-D heat balance equation for steady state conditions with a finite difference numerical solution. The temperature distribution is determined from the solution of the system of governing equations formed by the energy balance equation for conduction thermal mode. The analysis of temperature variation will be useful in the study of reliability and failure mechanism. The Fig. 7(a) shows the temperature variation when the membrane is in up position. (Hot in centre) The bridge is cool at supports and hot at centre. In the down position the bridge is cool at centre as shown in Fig. 7(b) because the membrane is in intimate contact with bottom electrode. The Frankel-Poole mechanism heavily depends on temperature and thus results in leakage current in the dielectric. Since dielectric used is silicon nitride which has high concentration of traps, eventually will result in charging of most of them.

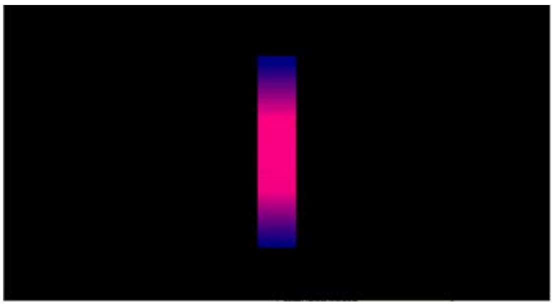

Fig. 7 (a) temperature variation of membrane (up position)

Fig. 7 (b) temperature variation of membrane (down position)

5 RF MEMS inductor

The parasitic capacitance between the inductor and the ground plane is a problem for planar inductors. Components such as inductors with high Quality factor Q (exceeding 25), which are required for high-frequency selectivity in communication systems can not be designed with conventional integrated circuit (IC) technology [23]. These parasitic, both lower the Q of the inductors and create a self-resonance frequency that limits the maximum frequency of operation, making the devices insufficient for communication applications. The large parasitic capacitance of a planar inter-digitated capacitor, which is directly related to the fabrication process, also affects the performance as a true lumped element. To improve the performance, MEMS inductors are proposed to be used high performance systems. The inductor is suspended above the substrate resulting in near to zero parasitic capacitance. A typical MEMS inductor meshed model generated by tool is shown in Fig. 8. A three-dimensional FEM based inductance extractor that is fast and accurate has been implemented.

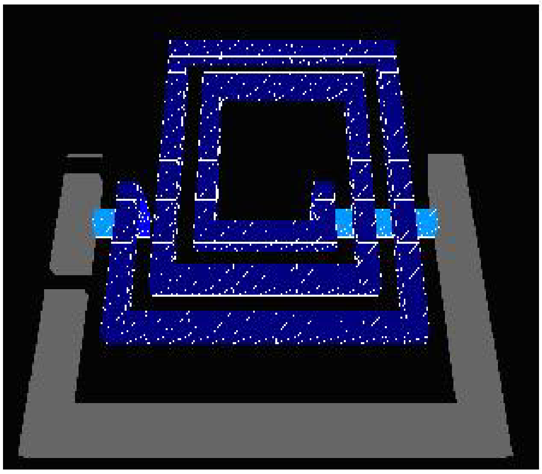

Fig. 8 Meshed model of RF MEMS inductor

The extractor is useful for developing and characterizing RF MEMS inductors. A three dimensional tetrahedral meshed model is generated by the tool. The nodal voltages are calculated by solving Laplace equation $\nabla^2 V = 0$ with iteration method using FEM followed by current density computations. The Finite Element Method can be effectively used to solve electrostatic problems [24][25]. The Laplace equation is solved using FEM. The homogeneous solution region i.e. the volume of inductor is divided into sub regions or elements. The tetrahedral meshing is considered here for analysis. For ease of computation the elements of same type are preferred throughout the region. Then we seek an approximation for the potential V_e within an element *e* and then interrelate the potential distribution in various elements such that the potential is continuous across inter element boundaries. The element coefficient matrices are calculated. The next step is to assemble all elements in the solution region. By carefully considering the global and local numbering the global coefficient matrix is obtained. The Laplace equation is satisfied when the total energy is minimum in the solution region. The partial derivatives of W_e with respect to each nodal value of the potential be zero, i.e.

$$\frac{\partial We}{\partial V_k} = 0, \qquad k = 1, 2, \cdots, n.$$

which leads to

$$0 = \sum_{i=1}^{n} V_i \, C_{ik}$$

.where n is the total number of nodes. Iteration method is employed to obtain the potential at each node. The fixed potentials are connected at both ends of the inductor. The potential at nodes of element are obtained. The potential obtained generate current density distribution inside the volume of the conductor. The energy of the resulting magnetic field is estimated by integration of Neumann's formula [26] [27]

$$W = \frac{\mu}{8\pi} \int_v \int_v \frac{\vec{J}(\vec{r}) \cdot \vec{J}(\vec{r}')}{|\vec{r} - \vec{r}'|} d^3r' \, d^3r \qquad \text{............ (3)}$$

where v denotes the volume of the conductor, r and r' denote locations in the volumes. Instead of evaluation of the magnetic vector potential

$$\vec{A}(\vec{r}) = \frac{\mu}{4\pi} \int_v \frac{\vec{J}(\vec{r})}{|\vec{r} - \vec{r}'|} d^3r'$$

and calculating

$$W = \frac{1}{2} \int_v \vec{A}(\vec{r}) \cdot \vec{J}(\vec{r}) \; d^3r$$

with the Gaussian integration scheme, Eq (3) is estimated by means of Monte Carlo sampling [27]

$$W \approx \frac{1}{N} \frac{\mu}{8\pi} \sum_i \frac{\vec{J}(\vec{r}) \cdot \vec{J}(\vec{r}_i')}{|\vec{r}_i - \vec{r}_i'|} \frac{1}{p^2 (\vec{r}_i, \vec{r}_i')}$$

$$= \frac{1}{N} \sum_i W_i \qquad \text{......... (4)}$$

During every sample i two locations $\vec{r}_i$ and $\vec{r}_i\,'$ are chosen randomly according to the probability density $p^2(\vec{r}\ ,\vec{r}\,')$>0. The probability density depends on both locations $\vec{r}_i$ and $\vec{r}_i\,'$ and has to be normalized [27] [28] [29]

$$\int_v \int_v p^2(\vec{r}\ ,\vec{r}\,')\, d^3r'\, d^3r \equiv 1 \qquad ....(5)$$

The inductance L is computed from W and the total current through a conductor with $W = (1/2)\, L\, I^2$.

A three turn aluminum inductor with cross section 85 µm x 20 µm and spacing 60 µm suspended above substrate shown in Fig 8 is analyzed for validation. The inductance offered by the device is 3.44 nH which is very close to experimentally observed value [30]. The current density distribution obtained and found is maximum at the inside corners which is expected. The effect of surface roughness is analyzed on scaled inductors with reduced surface to volume ratio of cross sections 65 µm x 20 µm, 50 µm x 20 µm, 20 µm x 20 µm and 3 µm x 20 µm with same length and same geometric mean distance. These values are chosen because most of the inductors are now fabricated in this range now days. The extracted inductances for smooth topology and with surface roughness 65 nm rms (fractal dimension D=1.58), are obtained. The sides of inductor are modeled as rough surfaces. The inductance extracted increases with reducing cross section, with the same length, which is also observed experimentally [30].

Table 1

Cross section (micrometer)	Inductance (nH) (smooth topology) L smooth	(65nm rms roughness) L rough
3x20	5.64	6.17
20x20	5.31	5.60
50x20	4.01	4.16
65x20	3.63	3.76
85x20	3.44	3.57

The inductances extracted with smooth topology and with 65 nm rms surface roughness are shown in Table 1.The inductance offered by the 3 micrometer x 20 micrometer cross section is 5.64 nH, which increases to 6.17 nH for 65 nm rms roughness. For 20 x 20 micrometer cross section the inductance reduces to 5.31 nH for smooth topology. For rough surface topology the inductance increases to 5.60 nH. For 85 x 20 micrometer the inductance offered for smooth topology is 3.44 nH, which increases to 3.57 nH with 65 nm rms roughness. The inductance is extracted for different values of rms roughness. The current flowing close to the surface is significantly affected by the rough profile. With increase in surface roughness the extracted inductance value increases. The increase in inductance is due to the increased circular current paths inside the volume [31].

6 Summary and Conclusion

In this paper CAD tool developed for RF MEMS shunt switch and RF MEMS inductor is presented. To design a MEMS based system and improve manufacturability, there is emergent need of a CAD system. The CAD for MEMS is a multiple energy domain suite of programs and essentially complex in nature. Due to complexity, the second order effects are not presently addressed by these tools. The discrepancy of measured and simulated results is reported for RF MEMS devices. To improve manufacturability, there is need for developing an efficient, accurate modeling and simulation computer programs for RF MEMS devices. The structured methodology is adopted in this work for development of modeling and simulation tool. The computer routines are developed for RF MEMS shunt switch and RF MEMS inductor. The device specific tool addresses the issues related to surface roughness. The effect of surface roughness on capacitance and maximum electric field is studied. The thermal analysis of RF MEMS switch is performed. The effect of surface roughness and temperature is useful in understanding failure mechanism and reliability issues. A 3-D FEM extractor with Monte-Carlo sampling is developed for MEMS inductor. The effect of surface roughness on inductance is studied. However, our work is limited to the extraction of RF MEMS inductor of fixed values. The analysis may be extended to variable RF MEMS inductors in future. The mechanical movement with applied electrostatic field may be considered for analysis.

The algorithm may be extended to extract inductances for complex structure. Recently the

inductors fabricated in carbon nano tube technology are reported. The extractor may be further developed for analysis of these inductors. The analysis of magnetic field vector at rough surfaces may be investigated in future.
For the ease of computations we have considered elements of equal size in FEM modeling. However the meshing should be denser where the change in parameter value is more. This will facilitate more values at specific location and more accurate results. The extractor developed may be extended for other RF MEMS devices. The efforts made by us to develop the modeling and simulation tool will be certainly useful for RF MEMS community.

References:

[1] Stephen D. Senturia, "CAD challenges for Microsensors, Microactuators and Microsystems," *Proceedings of the IEEE*, Vol. 86, No.8, August 1998, pp1611-1626.

[2] T.Ozdemir, K.F.Sabet, J.L.Ebel, G.L.Creech, L.P.B.Katehi, K.Sarabandi, "Numerical modeling of imperfect contacts in capacitively coupled RF MEMS switches." www.emagtech.com.

[3] J. R. Reid, *"RF MEMS for antenna applications,"* Short Course No. 9, IEEE AP-S *Intl.Symp.,Boston*, Massachussetts, June 2001.

[4] Gary K. Fedder, "Structured design of Integrated MEMS," *12th IEEE International conference on MEMS*, Jan 1999.

[5] M. Husak, J. Jakovenko, P. Kulha, Boura A., "Design of MEMS and Microsystems- Models and simulation," *WSEAS Transactions on systems,* Issue 5, Volume 4, May 2005, pp 635-644.

[6] John K. Sakellaris, "Finite element analysis of micro-Electro-Mechanical systems: Towards the integration of MEMS in design and robust optimal control schemes of smart microstructures," *WSEAS transactions on applied and theoretical mechanics,* March 2008, pp 114-124.

[7] Nicholas R. Swart, "A design flow for micro machined Electromechanical systems," *IEEE design and test of computers*, Oct-Dec 1999.

[8] John R.Gilbert, "Integrating CAD tools for MEMS design," *IEEE computer*,April 1998.

[9] www.opengl.org

[10] S.Mujamdar, M.Lampen, R.Morrison, J.Macial, "MEMS Switches," *IEEE Instrumentation & Measurement Magazine* March 2003 pp12-15.

[11] Elliott R. Brown, "RF-MEMS switches for reconfigurable Integrated circuits," *IEEE Transactions on microwave theory and techniques*, vol. 46, No. 11, November 1998, pp1868-1880.

[12] Rajesh S. Pande, R.M. Patrikar, "Finite element analysis and optimization of RF MEMS devices," *International conference on computer aided engineering*, IIT Madras India, Dec. 2007, pp 375-383.

[13] J. Jason Yao, "RF MEMS from a device perspective," *J.Micromech. Microeng.* Vol.10, pp.R9- R38. (2000).

[14] F. D. Flaviis and R. Coccioli, "Combined mechanical and electrical analysis of microelectromechanical switch for RF applications," *European Microwave Conference EUMC 1999*, Munich, Germany, 1999, pp.247-250.

[15] N. AbuGhalioun, H. Hassan, H. Ibrahim, "Analysis and parametric modeling of RF MEMS capacitive shunt switch," *Proceedings of the 11th conference on circuits*-Volume -11, pp 213-217.

[16] R.M.Patrikar, Chong Yi Dong, W.Zhuang, "*Modeling interconnects with surface roughness*," Microelectronics Journal 33,2002, pp 929-934.

[17] L.Lai, E.A.Irene, J.Vac. "Area evaluation of microscopically rough surface," *Sci.Technol.B* 17,1999, pp 33-39.

[18] Rajesh S. Pande, R.M. Patrikar, "Effect of surface roughness on RF MEMS shunt switch," *International conference on MEMS and semiconductor nanotechnology*, IIT Kharagpur, Dec 2005, India.

[19] Rajesh Pande, Rajendra Patrikar, "A CAD tool for RF MEMS devices," 13th *Asia and south pacific design automation conference*, ASP-DAC 2008, Seoul, Korea, pp 89-94.

[20] C. Goldsmith et al. "Lifetime characterization of capacitive RF MEMS switches," *IEEE Int. Microwave Theory and Techniques Symp.*, Phoenix, AZ, May 2001.

[21] Jonathan Lueke et al. "A Parametric Study of Thermal Effects on the Reliability of RF MEMS Switches," International Conference on MEMS, NANO and Smart Systems, July 2005, IEEE Computer Society.

[22] Brian D. Jensen et al "Fully integrated electro thermal multiple modeling of RF MEMS switches," IEEE *microwave and wireless component letters*, vol. 13, no. 9, September 2003.

[23] Amal Zaki, "Design and fabrication of high-Q spiral inductors using MEMS technology,"

WSEAS transactions on Electronics, Issue 8, Volume 3, August 2006, pp 432-436.

[24] M.N.O. Sadiku, "A simple introduction to finite element analysis of electromagnetic problems," *IEEE Trans. Educ*., vol.32, no.2, May 1989, pp. 85-93.

[25] P.P. Silvester and R.L. Ferrari, *Finite elements for Electrical engineers*, *Cambridge*, Cambridge University press, 1983.

[26] F. Grover, *Inductance calculations,* Dover Phoenix edition, 1973.

[27] R.Rubinstein, *Simulation and the Monte-carlo Method,* J.Wiley & sons.1981.

[28] C.Hoer, C.Love, "Exact inductance equations for Rectangular Conductors with Applications to More Complicated Geometries," *Journal of research of National Bureau of Standards*, 69C,1965, pp127-137.

[29] G.Leonhardt, W.Fichtner, "Acceleration of Inductance Extraction by means of Monte Carlo Method Integrated systems laboratory," *Swiss Federal Institute of Technology, Gloriastr 35*, 8092 Zurich, Switzerland.

[30] Vijay K. Varadan, K.J.Vinoy and K.A. Jose, *RF MEMS and Their Applications*, John Wiley & Sons, Ltd. 2003.

[31] Rajesh S. Pande, A. Jalgaonkar, R.M. Patrikar, "A 3-D FEM based extractor for MEMS inductor with Monte-Carlo sampling," XIV *International workshop on physics of semiconductor devices, IWPSD,* Dec. 2007, IIT Bombay, India.